

# Variable Structure-Based Control for Dynamic Temperature Setpoint Regulation in Hospital Extreme Healthcare Zones

Ali Hamza <sup>1</sup>, Muhammad Uneeb <sup>2</sup>, Iftikhar Ahmad <sup>2</sup>, Komal Saleem <sup>1</sup> and Zunaib Ali <sup>1,\*</sup>

<sup>1</sup> London Center of Energy Engineering (LCEE), School of Engineering, London South Bank University, London SE1 0AA, UK; hamzaa10@lsbu.ac.uk (A.H.); saleemk2@lsbu.ac.uk (K.S.)

<sup>2</sup> Department of Electrical Engineering, School of Electrical Engineering and Computer Science, National University of Sciences and Technology (NUST), Islamabad, Pakistan; muneeb.msee17seecs@seecs.edu.pk (M.U.); iftikhar.rana@seecs.edu.pk (I.A.)

\* Correspondence: aliz29@lsbu.ac.uk

**Abstract:** In critical healthcare units, such as operation theaters and intensive care units, healthcare workers require specific temperature environments at different stages of an operation, which depends upon the condition of the patient and the requirements of the surgical procedures. Therefore, the need for a dynamically controlled temperature environment and the availability of the required heating/cooling electric power is relatively more necessary for the provision of a better healthcare environment as compared to other commercial and residential buildings, where only comfortable room temperature is required. In order to establish a dynamic temperature zone, a setpoint regulator is required that can control the zone temperature with a fast dynamic response, little overshoot, and a low settling time. Thus, two zone temperature regulators have been proposed in this article, including double integral sliding mode control (DISMC) and integral terminal sliding mode control (ITSMC). A realistic scenario of a hospital operation theater is considered for evaluating their responses and performance to desired temperature setpoints. The performance analysis and superiority of the proposed controllers have been established by comparison with an already installed Johnson temperature controller (JTC) for various time spans and specific environmental conditions that require setpoints based on doctors' and patients' desires. The proposed controllers showed minimal overshoot and a fast settling response, making them ideal controllers for operation theater (OT) zone temperature control.

**Keywords:** temperature environment; dynamics setpoints; HVAC; sliding mode control; operation room; thermal model



**Citation:** Hamza, A.; Uneeb, M.; Ahmad, I.; Saleem, K.; Ali, Z. Variable Structure-Based Control for Dynamic Temperature Setpoint Regulation in Hospital Extreme Healthcare Zones. *Energies* **2023**, *16*, 4223. <https://doi.org/10.3390/en16104223>

Academic Editors: Li Yang and Anastassios M. Stamatelos

Received: 17 March 2023

Revised: 17 May 2023

Accepted: 18 May 2023

Published: 20 May 2023



**Copyright:** © 2023 by the authors. Licensee MDPI, Basel, Switzerland. This article is an open access article distributed under the terms and conditions of the Creative Commons Attribution (CC BY) license (<https://creativecommons.org/licenses/by/4.0/>).

## 1. Introduction

During recent decades, the amount of research on constructing smart energy-conserving buildings has increased [1]. Scientists and engineers are making efforts to understand and control the dynamic needs of energy for buildings. According to the International Energy Agency (IEA) [2], about 32% of total generated energy is consumed by buildings, which include residential apartments and offices, and more than 40% of this energy is used for space heating purposes. In European countries, during winter, the temperature is mostly low, and thus, the energy consumption for space heating increases. This demand for heating load goes even higher in Scandinavian countries. Thus, to fulfill these needs, fossil fuels are used for energy generation, resulting in a huge amount of CO<sub>2</sub> emissions. In general, various parameters such as the thermal model of buildings, ventilation, climatic conditions, and end-consumers affect residential and official building energy loads [3]. Due to these factors, the average power consumption increases by more than 200  $\frac{\text{KWh}}{\text{m}^2}$  every year in the European Union [4]. Therefore, it is imperative to take bold steps for conserving energy in offices and residential buildings. Heating, ventilation, and air conditioning (HVAC) systems are used to regulate the temperature and humidity ratio as well as to provide

thermal comfort to the occupants. The most energy intensive application in a commercial building is the HVAC system, consuming around 40% of the total energy consumption of the building [5,6]. Thus, the efficiency of HVAC should be increased in order to minimize energy consumption while maintaining thermal comfort, and to this end, energy management plays a vital role.

To fulfill the growing needs for energy, various energy load models for buildings have been proposed [7]. The mathematical modeling of dynamic heat load for a given building is a complex task, as it requires considering several dependent parameters that could affect the heat load. The parameters associated with environmental conditions, building materials, and habitats of the buildings are all nonlinear complex numerical functions that add complexity to thermal building models [3,8,9]. Three techniques are used to model the thermal load behavior for buildings including offices, schools, residential apartments, and hospitals: the physical model or “white box” technique, the statistical or machine learning “black box” technique, and the hybrid or “grey box” technique [10]. In the white box technique, a physical model of the building is formulated considering all of the variables involved in the thermal behavior of the building. Computational fluid dynamics (CFD), zonal, and multi-zonal are types of physical model techniques. In case of limited information about the heat transfer equation, and thermal and geometrical parameters of the building, the heat load can be predicted by statistical methods. The black box is formed by using sample data that describes the behavior of the system. In the black box, the parameters are generally adjusted automatically [11]. The third category is a hybrid method (grey box), which uses both physical and statistical modeling techniques [12]. These models perform well even if the building parameters are unknown and depend on sample data collected from the site, which, however, is a difficult task. A number of different statistical techniques have been proposed to predict the heat load for different cases. Some of these are, artificial neural networks (ANNs), genetic algorithms, linear multiple regression, and support vector machine (SVM) [13–16].

A building’s energy performance is commonly evaluated by the steady-state models. A study using the Overall Thermal Transfer Value (OTTV) method [17] has been carried out to understand the effect of several building envelopes in different climate zones. However, the effect of inertia in building envelopes has been neglected. To overcome this problem, steady-state models have been proposed which include approximated effects of inertia. Depending on the envelope characteristics of the building, these models introduced several correction factors in the approximated inertia effects [18]. The drawback of steady-state models is the exclusion of evaluation of new technologies exploiting the building’s inertia effects such as phase change materials and free cooling. In this case, the only model that can be modified to analyze creative energy-saving alternative solutions is the transient dynamic model. Therefore, to forecast the energy performance of a building, a thermal model comprising of Thermal Resistance (R) and Capacitance (C) (electrical network analogy) has been introduced in [19]. Several numerical approaches have been developed, analyzed, and executed in software like DOE-2, EnergyPlus and many more [20,21]. However, the MATLAB/Simulink environment is a better option for performing dynamic building simulations without excessive computational costs and with a satisfactory level of accuracy.

The most important goal in HVAC installation is to design an effective control strategy for meeting thermal comfort while keeping the energy consumption of the devices to a minimum. Various control strategies have been implemented for HVAC [22]. Proportional integral derivative (PID) controllers, based on the Ziegler–Nichols (ZN) method, have been implemented in an HVAC dynamic model in [23] for reducing disturbances and improving indoor comfort. Due to the linearity of PID controllers, using them for a nonlinear system such as HVAC causes degraded performance. In the case of model nonlinearities and system uncertainties, robust control perhaps would be useful [22]. In Ref. [24], a multi input multi output (MIMO) robust controller is used for HVAC, which offers improvement in the system with disturbance rejection compared to a proportional plus integral (PI) controller. Model predictive control (MPC) has also gained popularity

for HVAC applications [25–27]. A supervisory setpoint control optimizer based on MPC is coupled with a digital parameter-adaptive controller and used in a demand response system [6]. It performed better than the classical control methods and adaptive fuzzy neural control [28]. A three-layered ANN has been proposed to predict the energy and heat load of a building [29,30], where sample data are collected by using a DOE-2 simulation for training the statistical model. A similar ANN with two hidden layers is used to predict the heat load for a building in [30]. Sample data of 80 and 170 values for two different rooms are used to train the ML algorithm, and an accuracy of 90% is achieved. The use of statistical models for prediction has certain advantages in gathering dynamic information for any system. The design of the predictive model does not require knowledge of any system parameter and requires only collecting samples for training the neural network. However, due to the black box model approach, the actual system model and parameters remain unknown and cannot be changed. Also, it is very difficult to collect the training data with the help of observations, sensors, or numerical calculations which may result in poor performance in case of a large variance in the training sample or if the training sample is small.

Controller design for HVAC poses several challenges due to the nonlinear, complex and MIMO features. It has time-varying and inherent parameter coupling effects [28,31,32]. Variations in system parameters, model uncertainty due to nonlinear factors, climatic parameters interaction, and variable conditions are some of the major issues faced by HVAC systems. As a result, linear control algorithms are inadequate in terms of performance and stability when dealing with the nonlinearity behavior of the system. Therefore, it is essential to implement nonlinear control algorithms to address the aforementioned issues. Sliding mode control (SMC)-based approaches show promising results for various nonlinear systems. To regulate the superheat temperature of the evaporator in HVAC, a feedback linearization-based SMC controller is presented in [33]. An SMC and PID approach has been designed for optimization of building energy consumption in [34] for a multizone VAV air-conditioning system. Robust SMC and PID have been implemented to ensure the robust performance of the air handling unit in the presence of uncertainties [35]. The authors in [36] demonstrated a super-twisting SMC for the control of an HVAC system evaporator two-phase length and superheat temperature. However, the stability analysis prevents the super-twisting approach from being implemented [37]. Hotel energy analysis [38], Soft Actor-Critic Agent and predictive mean vote index for enhancement of indoor temperature and energy saving in the building have been implemented [39,40]. The work in our paper proposes advanced and stable SMC controllers for a hospital HVAC system.

Noteworthy, HVAC system for hospital requires a specialized approach due to unique need of medical facilities. In addition to providing thermal comfort, factor such a patients well being, safety, cooling of specialized surgical equipment, control of precise temperature and humidity are critical. Prioritizing patient comfort and recovery while ensuring medical equipment efficiency is essential. People suffering from the medical condition deserve the best thermal comfort possible to assist them on their healing journey. Hence, temperature and humidity control is fundamental.

This paper selected a special case of a hospital building, considered as a complex organization among various commercial buildings in the sense of its operations, biomedical technology, and healthcare procedures. In modern hospitals, occupants' comfort and maintenance of controlled environmental conditions for machinery and other medical equipment have become a necessity, which is achieved by installing HVAC systems as per medical standards. However, such facilities can only be ensured at the cost of high energy consumption, which is identified as the third largest factor among other expenditures in the healthcare sector after staff salaries and medicines. It was also revealed that most of the electricity is consumed for air conditioning, which is more than 50% of the total electricity demand of the building. The highest energy use intensity (EUI) value was found for the hospital's critical area, i.e., operation theaters (OTs). In OTs, the EUI value is about three times higher than in the other areas and offices in the hospital [41]. Thus, it is pertinent to

have energy management and controlling algorithms to efficiently manage the heating and cooling processes.

The energy management of a healthcare building is a crucial and complex task for researchers due to uncertainty, and thus, various load prediction models are applied to supply uninterruptible supply to the healthcare building. In this paper, a deterministic model for zone temperature has been proposed. The following are the aims and control objectives:

- For the case of intensive care units (ICU) and OTs in a hospital environment, dynamic setpoints for the zone temperature are incorporated.
- The model will be processed on the dynamic temperature setpoints of operation rooms (ORs) inside the hospital. This is because, in ORs, both patients and healthcare workers desire different temperature environments depending on the patient's condition and the requirements of the surgical and treatment procedures.
- To achieve the dynamic setpoints' variability, a detailed mathematical model of the zone temperature is considered in the formulation of the controller.
- The major influencing parameters of the internal zone temperature, i.e., outside air temperature, solar irradiation, wind speed, and heat generated from internal appliances are incorporated into the design of the controller.
- For the dynamic regulation of the HVAC temperature, two nonlinear controllers, DISMC and ITSMC, have been proposed.
- Asymptotic stability of the system has been ensured for both nonlinear controllers.

The paper is organized as follows: The mathematical model of heating load demand is explained in Section 3. The controller designs are presented in Section 4 and simulation results are analyzed and discussed in Section 5. Section 6 details the conclusions with future work.

## 2. Hospital Case Study

In this research, an OT in Shifa International Hospital (SIH), situated in Islamabad Capital Territory (ICT), Pakistan, is considered as the case study. The hospital building has a 550-bed operational capacity and falls in the quaternary category. SIH is a Joint Commission International (JCI) certified hospital that provides its services to national as well as international patients due to its best performance and high-tech environment. A vast variety of complex major and minor operation procedures can be conducted in the ORs situated at the SIH facility. To carry out complex procedures, SIH has fully equipped and state-of-the-art operational facilities. The major operations performed at the SIH facilities include heart bypass surgery, liver transplants, corneal transplants, bone marrow transplants, total knee replacement, and neurosurgery. The OR section is shown in Figure 1 and a complete layout plan of the ORs floor is presented in the Appendix A. The selected zone for this research is OR-14. The internal view of the selected OR is presented in Figure A1, given in the Appendix A.



**Figure 1.** General view of OR, HVAC ducts, and corridor of hospital. (a) OR corridor 1; (b) OR corridor 2; (c) OR; (d) HVAC ducts.

### 3. Thermal Mathematical Model

The internal layer of the walls exchanges heat with the external air through the wall and windows. This isothermal volume receives free heat gain from the internal human and heat-radiating appliances. The whole OR is represented in a parallelepiped structure with squared floors, having an internal volume of  $310.6677 \text{ m}^3$  with unique thermal capacitance. The OR model consists of four external wall portions including east, west, north, and south walls. The dynamical equation of the roof is also considered to represent the contribution of external temperature to the internal air of the OR. At the south wall, the window has an accumulated surface area of  $6.25 \text{ m}^2$ . All of the dimensions of the OR are mentioned in Table 1. Heat transfer is also taken into account due to ventilation and direct solar radiation through the window. The heavy and light configurations of the wall structure of the OR are also considered, which differ from each other on the basis of their thermal capacitance and the mass of the vertical walls and roof. Table 2 presents the thermal transmittance and thermal capacity for the heavy and light walls of the OT, including the values for the roofs and floors.

**Table 1.** Geometric values for the OR.

|   |                 |                  |
|---|-----------------|------------------|
| Height                                      | m               | 4                |
| Base  | m × m           | 11.5824 × 6.7056 |
| Number of Floors                            | -               | 1                |
| Volume                                      | m <sup>3</sup>  | 310.6677         |
| Surface-to-Volume Ratio (S/V)               | m <sup>-1</sup> | 0.73             |
| Roof Surface                                | m <sup>2</sup>  | 77.6669          |
| Type of Floor                               | -               | On First Floor   |
| Vertical Wall Orientation                   | -               | N – S – E – W    |
| <b>For Each Orientation</b>                 |                 |                  |
| Total Opaque Wall Surface Area (East, West) | m <sup>2</sup>  | 46.3296          |
| Total Opaque Wall Surface Area (East, West) | m <sup>2</sup>  | 26.8224          |
| Opaque Wall Surface Area (South)            | m <sup>2</sup>  | 21.8224          |
| Window Surface (South)                      | m <sup>2</sup>  | 5                |

**Table 2.** Wall structure parametric values.

| Thermal Transmittance (W m <sup>-1</sup> K <sup>-1</sup> ) |      | Specific Thermal Capacity (kJ m <sup>-2</sup> K <sup>-1</sup> ) |
|--|------|---|
| <b>Heavy Wall</b>  |      |   |
| Vertical Wall  | 0.40 | 622.92  |
| Roof   | 0.35 | 395.28  |
| Floor  | 0.42 | 320.65  |
| <b>Light Wall</b>  |      |   |
| Vertical Wall  | 0.40 | 39.47   |
| Roof   | 0.35 | 298.58  |
| Floor  | 0.42 | 320.65  |

The block diagram of the OR is shown in Figure 2, where solar radiation from the Sun contributes to the internal air temperature through the transparent window surface and the opaque surface of the wall. Let  $\dot{x}_{win}$  be the flow of heat charge across the window.  $\dot{x}_{sg}$  represents the thermal energy contribution due to solar radiation. Heat transfer to the wall is represented by  $\dot{x}_{wl}$  due to internal and external temperature differences.  $\dot{x}_{hs}$  and  $\dot{x}_{cs}$  are the dynamic inputs of the HVAC source, with efficiency  $\eta$ , which depends on the system's performance, external conditions, and regulation criteria. The internal free heat gain due to people and equipment is represented by  $\dot{x}_{is}$ , as shown in Figure 2.  $\dot{x}_v$  refers to the heat transfer through the windows due to ventilation. The blue lines in the block diagram show the cooling input whereas the red lines represent the heating input to the internal air temperature. The dynamic evolution of the internal air temperature [19] is presented as:

$$C_{OR} \frac{dT_{OR}}{dt} = \dot{x}_{hs/cs} + \dot{x}_{is} + \dot{x}_v + \dot{x}_w + \dot{x}_{win} \quad (1)$$

where  $C_{OR}$  is the total capacitance of the OR including the thermal capacities of the walls, window glass, and roof of the OR.  $T_{OR}$  is the internal air temperature, which is the accumulative effect of all of the aforementioned factors.  $C_{OR}$  is the thermal capacitance depending upon the material used for the OR and its properties vary from material to material.

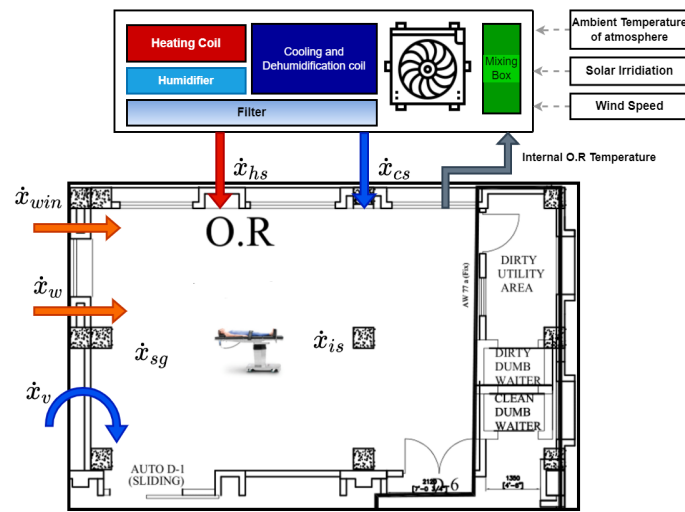


Figure 2. Block diagram of OR heat transfer with the HVAC system.

3.1. External Walls

There are two layers for each wall, one is an internal layer and the other is an external layer. The mass of internal air is in direct contact with the inside layer of the wall. The main contributors to the internal air temperature are heat sources, electrical appliances radiating heat, and the human body temperature present inside. The external layer is the layer that is subjected to the environmental effect, including solar irradiation and external air temperature.

Radiation coming from the Sun is directly absorbed by the wall contributing to the rise in temperature and some passes through the transparent surface of the window, causing an increase in the internal temperature. The wall temperature is considered at a single point inside the wall and that point can be close to the internal wall or to the external wall depending on the material and insulation used. The total temperature of the wall is considered as a temperature difference between the internal and external walls.

The transient energy of an opaque external wall can be written as follows:

$$C_{w,j} \frac{dT_{w,j}}{dt} = \dot{x}_{wi,j} + \dot{x}_{we,j} \tag{2}$$

where  $C_{w,j}$  represents the total thermal capacitance of the wall and  $T_{w,j}$  is the temperature of the wall’s internal node. The flow of heat flux from the external layer towards the wall node and the flow of heat flux from the internal layer towards the wall node are represented by  $\dot{x}_{we,j}$  and  $\dot{q}_{wi,j}$ , respectively, and can be calculated as follows:

$$\dot{x}_{wi,j} = \frac{(T_{wi,j} - T_{w,j})}{R_{wi,j}} \tag{3}$$

$$\dot{x}_{we,j} = \frac{(T_{we,j} - T_{w,j})}{R_{we,j}} \tag{4}$$

where  $T_{wi,j}$  and  $T_{we,j}$  are the internal layer and external layer temperatures of the wall, respectively.  $R_{we,j}$  and  $R_{wi,j}$  are the thermal resistance to the flow of heat flux from the external layer and internal layer to the wall node, respectively, which is purely conductive and its values are known depending upon the nature of the wall material. In the case of a heavy wall structure, this resistance is high and prevents sudden internal changes in case of a change in environmental conditions. When modeling the wall, there is a need to consider the effect of solar radiation coming inside through the windows and reflecting from the floor.

As the deterministic model approach is used, and the values of the internal and external wall layer temperatures  $T_{wij}$  and  $T_{wej}$  cannot be calculated directly by using sensors, the values of these wall layer temperatures can be determined by considering the two energy balance equations given below:

$$\dot{x}_{wi,j} + \dot{x}_{sg,j} = \dot{x}_{i,j} \quad (5)$$

$$\dot{x}_{we,j} + \dot{x}_{s,j} = \dot{x}_{e,j} \quad (6)$$

where  $\dot{x}_{sg,j}$  and  $\dot{x}_{s,j}$  are the solar contributions and will be explained in a later section.  $\dot{x}_{i,j}$  and  $\dot{x}_{e,j}$  are the total heat flux flows on the internal and external wall surfaces, respectively.

### 3.2. Solar Contributions

The heat contribution from the Sun's radiation is divided into two parts, heat absorbed by the wall's opaque surface and transmittance of solar radiation through the windows. The heat flux absorbed in the surface of the wall can be expressed as follows:

$$\dot{x}_{s,j} = \psi_{w,j} S_{w,j} I_{j,n} \quad (7)$$

where  $\psi_{w,j}$  is the wall absorbance coefficient, which depends on the external surface of the wall  $j^{th}$ .  $S_{w,j}$  is the total opaque surface area of wall and  $I_{j,n}$  is the amount of solar radiation normal to the  $j^{th}$  wall and taken from weather data.

The total solar radiation transmitted through the transparent surface of glass windows can be modeled as:

$$\dot{x}_{sg} = \sum_j f_j S_{w,j} I_{j,n} \tau_{win,j} \quad (8)$$

where  $\tau_{win,j}$  is the transmittance coefficient of the window glass and  $S_{w,j}$  is the total transparent surface area of the window.  $f_j$  is the function of shadow on the window depending upon the orientation of the Sun. Some amount of solar radiation passes from the window and is absorbed by the floor depending on the absorption coefficient  $\psi_{fl}$  and can be modeled as:

$$\dot{x}_{sg,f} = \psi_{fl} \dot{x}_{sg} \quad (9)$$

The rest of the solar radiation is reflected from the surface of the floor and considered as uniformly distributed in the internal air volume and can be modeled as:

$$\dot{x}_{sg,j} = \frac{S_{w,j}}{\sum_j S_{w,j}} (1 - \psi_{fl}) \dot{x}_{sg} \quad (10)$$

where  $I_{j,n}$  is the global solar radiation normal to the surface of the wall.

### 3.3. Ventilation

The heat transfers across walls either due to the presence of a ventilation system in the form of windows or through the air-conditioning exhaust system. The heat flux through the ventilation system [8] can be modeled as:

$$M_v c_{vv} \frac{dT_v}{dt} = U_v (T_{OR} - T_v) \quad (11)$$

$$U_v = \rho_a \dot{v}_a c_a \quad (12)$$

where  $U_v$  is the overall heat transfer coefficient and  $\dot{v}_a$  is the air volume conditioned per minute.  $\rho_a$  and  $c_a$  are the density and specific heat of the air, respectively.  $M_v$  is the mass,  $c_{vv}$  is the specific heat, and  $T_v$  is the temperature of the ventilation system.

### 3.4. Windows

Heat flux flows across the windows due to the difference between the internal and external temperatures, and can be modeled as an energy balance equation:

$$\dot{x}_{win} = (T_e - T_{OR}) \sum_j U_{win,j} S_{win,j} = \frac{(T_e - T_{OR})}{\sum_j R_{win,j}} \quad (13)$$

The total heat flux flowing across the window depends on the temperature difference between the external and OR temperatures and the resistance of the window glass. This resistance can also be modeled as the inverse of the transmittance of glass across the total transparent surface area  $S_{win,j}$  of the window.  $U_{win,j}$  is the transmittance of the windows, which depends upon the characteristics of the glass.

### 3.5. Humans and Applications

The contribution of heat flux to the internal air temperature due to the presence of humans and applications is considered as a constant that does not vary significantly with time, and its value is taken as 50 W.

## 4. Robust Controller Design

Sliding mode control (SMC) is a nonlinear control technique that presents high accuracy, low steady-state error (SSE), and robustness against model uncertainties and disturbances. It is relatively easy to implement and shows finite time convergence as compared to other nonlinear control techniques [42]. Various methods such as sliding surface design modification, high order SMC and composite SMC designs have been proposed to improve the conventional SMC performance in terms of reducing the chattering effect, rejecting disturbances, and tracking properties.

It presents a higher degree of flexibility in the designing process as compared to other controllers. It is an effective control strategy to force the system's state trajectories from the initial states to some predefined sliding surface using control law. Higher-order SMCs such as ITSMC and DISMC eliminate the reaching phase and improve the convergence time and robustness of the system [43]. ITSMC has dominant properties over SMC in terms of high state tracking accuracy and removal of chattering. For precision control, ITSMC is more relevant and its speed of convergence is quite near the equilibrium points. Thus, in this paper, DISMC and ITSMC are formulated and proposed for controlling the temperature of the nonlinear HVAC system.

The block diagram for SMC-based OR HVAC control is presented in Figure 3. To track the heating and cooling demand and supply, an error has been introduced into the system by taking the difference between the internal temperature of the OR and the dynamic zone temperature setpoints. A control input law that is based on nonlinear SMC is implemented to achieve the desired different temperature environments depending on the patient's condition and the requirements of surgical and treatment procedures. The mathematical evaluation of the control input law is presented in the subsequent sections.

In SMC, first of all, a sliding manifold ( $S = 0$ ) is defined to meet the control objectives and then a control law is formulated to constrain the motion of the system dynamics to the predefined sliding surface. Once the system dynamics reach the manifold  $S$  in finite time, it remains there because of the binary (0 and 1) switching states, as shown in Figure 4.

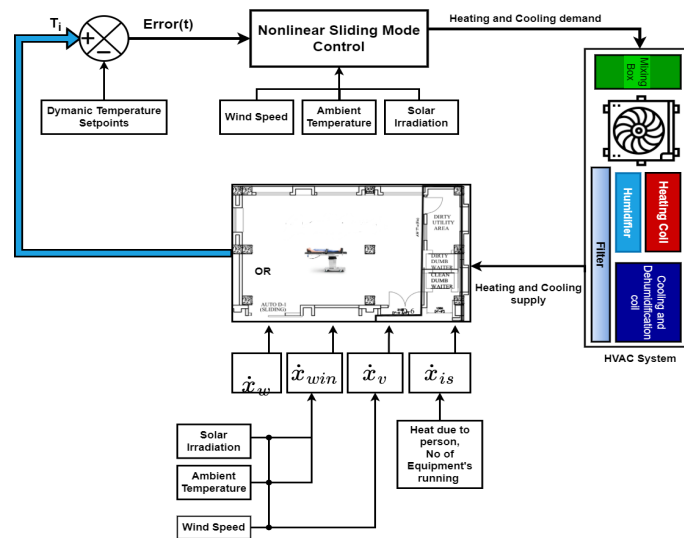


Figure 3. Block diagram of SMC-based HVAC control.

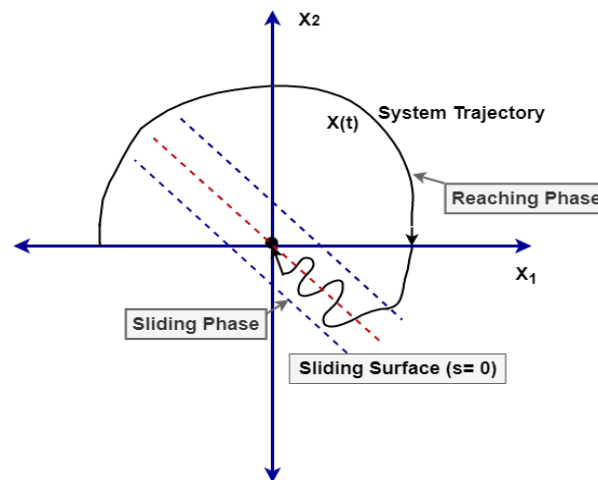


Figure 4. Phase plane diagram of SMC.

The sliding coefficient is used to control the convergence rate of the trajectory toward the sliding manifold. The reachability condition must be satisfied for guaranteeing convergence to the sliding surface. This condition states that the product of the sliding manifold and its derivative must be negative definite [42] as:

$$S \dot{S} < 0 \tag{14}$$

Due to the 0 and 1 switching states, chattering phenomena are observed in SMC. To reduce this chattering, a strong reachability condition is used to design the control law by considering:

$$\dot{S}_i = -K |S_i|^\alpha \text{sign} \left( \frac{S_i}{\phi_i} \right) \tag{15}$$

where  $\alpha$  is a unit between 0 and 1,  $|S_i|^\alpha$  in the expression of  $\dot{S}_i$  increases the speed of the trajectory toward the sliding manifold, and  $\phi_i$  is a small number used to reduce the chattering [44].

The sliding surface for a general multi input multi output (MIMO) system is defined as:

$$S = [S_1, S_2, \dots, S_n]^T \tag{16}$$

$S_1, S_2$ , up to  $S_n$  are the sliding surfaces for different outputs.

#### 4.1. Double Integral Sliding Mode Controller Design

The closed-loop response in SMC is totally unresponsive to external disturbances and internal parametric uncertainties. In order to improve the system convergence accuracy and reduce the SSE, integral action is required. A double integral has been added to the sliding surface to compensate for residual SSE and mitigate the chattering. Consider the following sliding surfaces:

$$S_1 = a_1 e_1 + a_2 e_2 + a_3 e_3 \quad (17)$$

where  $a_1, a_2$ , and  $a_3$  are sliding coefficients.  $e_2$  is the integral error in  $e_1$ .  $e_3$  is the double integral error in  $e_1$ . The second integral has been added to the sliding manifold to compensate for the remaining SSE and mitigate the chattering. In mathematical form, the errors are expressed as:

$$e_1 = T_{OR} - T_{OR_{ref}} \quad (18)$$

where  $T_{OR}$  is the operation theater room temperature and  $T_{OR_{ref}}$  is the reference temperature (desired).

$$e_2 = \int (T_{OR} - T_{OR_{ref}}) dt \quad (19)$$

$$e_3 = \int \left\{ \int (T_{OR} - T_{OR_{ref}}) dt \right\} dt \quad (20)$$

Now, the time derivative of the sliding manifold  $S_1$  is

$$\dot{S}_1 = a_1 \dot{e}_1 + a_2 \dot{e}_2 + a_3 \dot{e}_3 \quad (21)$$

To find the values of  $\dot{e}_2$  and  $\dot{e}_3$ , take the time derivative of (20) and (21) as:

$$\dot{e}_2 = \int (T_{OR} - T_{OR_{ref}}) dt = e_1 \quad (22)$$

$$\dot{e}_3 = \int \left\{ \int (T_{OR} - T_{OR_{ref}}) dt \right\} dt = e_2 \quad (23)$$

Substituting  $\dot{S}_1$  from (15) for  $i = 1$  and the derivative of errors in (18):

$$-K_1 |S_1|^\alpha \text{sign} \left( \frac{S_1}{\phi_1} \right) = a_1 (\dot{T}_{OR} - \dot{T}_{OR_{ref}}) + a_2 e_1 + a_3 e_2 \quad (24)$$

The use of  $\dot{T}_{OR}$  from (1) in (24) would result in:

$$-K_1 |S_1|^\alpha \text{sign} \left( \frac{S_1}{\phi_1} \right) = \frac{a_1}{C_{OR}} \left[ \dot{x}_{hs/cs} + \dot{x}_{is} + \dot{x}_v + \dot{x}_w + \dot{x}_{win} - \dot{T}_{OR_{ref}} C_{OR} \right] + a_2 e_1 + a_3 e_2 \quad (25)$$

Finally, solving (25) for HVAC control gives:

$$\dot{x}_{hs/cs} = -[\dot{x}_v + \dot{x}_w + \dot{x}_{win} + \dot{x}_{is}] + \dot{T}_{ORref} C_{OR} - \frac{C_{OR} a_2 e_1}{a_1} - \frac{C_{OR} a_3 e_2}{a_1} - \frac{C_{OR}}{a_1} [-K_1 |S_1|^\alpha \text{sign}(\frac{S_1}{\phi_1})] \tag{26}$$

For the stability of the sliding manifold of  $S_1$ , the Lyapunov candidate function is considered as

$$V_1 = \frac{1}{2} S_1^2 \tag{27}$$

By taking the time derivative of (27) and substituting  $\dot{S}_1$  from (15) for  $i = 1$  yields:

$$\dot{V}_1 = S_1 \dot{S}_1 = S_1 \left( -K_1 |S_1|^\alpha \text{sign}(\frac{S_1}{\phi_1}) \right) \tag{28}$$

The expression in (28) for  $i = 1$  becomes:

$$\dot{V}_1 = -K_1 |S_1|^\alpha \phi_1 \left| \frac{S_1}{\phi_1} \right| = -K_1 |S_1|^\alpha \phi_1 \frac{|S_1|}{\phi_1} \tag{29}$$

For  $|\phi_1| = \phi_1 = \phi$  and  $\phi_1 > 0$ , (29) results in:

$$\dot{V}_1 = -K_1 |S_1|^{\alpha+1} \tag{30}$$

As the derivative of the Lyapunov candidate function  $\dot{V}_1$  given by (30) is negative definite, this shows that the controller is stable.

#### 4.2. Integral Terminal Sliding Mode Controller Design

The DISMC lacks fast and accurate tracking of the dynamic changes in the reference input and thus, for precision control, ITSMC is more suitable and its speed of convergence is quite near the equilibrium points. In order to eliminate the singularity problem and to achieve high state accuracy tracking, integral terminal SMC has been proposed.

Defining the ITSMC sliding manifold as follows:

$$S_2 = e_1 + \kappa_2 \left[ \int_0^t e_1 dt \right]^{\lambda_2} \tag{31}$$

where  $\kappa_2$  is the design parameter of the sliding manifold and  $\lambda_2$  is a positive number such that  $1 < \lambda_2 < 2$ .  $e_1$  is the tracking error in the actual  $T_{OR}$  and the reference OR temperature  $T_{ORref}$ . Taking the time derivative of the sliding manifold and substituting  $e_1$  from (18) gives:

$$\dot{S}_2 = (\dot{T}_{OR} - \dot{T}_{ORref}) + \kappa_2 (\lambda_2) e_1 \left[ \int_0^t e_1 dt \right]^{\lambda_2-1} \tag{32}$$

Further, substituting  $\dot{T}_{OR}$  from (1) into (32) results in:

$$\dot{S}_2 = \dot{x}_{hs/cs} + \dot{x}_{is} + \dot{x}_v + \dot{x}_w + \dot{x}_{win} - \dot{T}_{ORref} C_{OR} + \kappa_2 (\lambda_2) e_1 \left[ \int_0^t e_1 dt \right]^{\lambda_2-1} \tag{33}$$

Solving (33) for the control input  $\dot{x}_{hs/cs}$  yields:

$$\dot{x}_{hs/cs} = -[\dot{x}_v + \dot{x}_w + \dot{x}_{win} + \dot{x}_{is}] + C_{OR} \dot{T}_{ORref} - C_{OR} \left[ -K_2 |S_2|^\alpha \text{sign}\left(\frac{S_2}{\phi_2}\right) - \left[ C_{OR} \kappa_2 \int_0^t e_1 dt \right]^{\lambda_2-1} \right] \quad (34)$$

For the stability of the sliding manifold  $S_2$ , taking the Lyapunov candidate function as:

$$V_2 = \frac{1}{2} S_2^2 \quad (35)$$

Taking the time derivative of (35) yields:

$$\dot{V}_2 = S_2 \dot{S}_2 \quad (36)$$

Putting  $\dot{S}_2$  into (36) gives:

$$\dot{V}_2 = -S_2 \left( K_2 |S_2|^\alpha \text{sign}\left(\frac{S_2}{\phi_2}\right) \right) \quad (37)$$

As the derivative of the Lyapunov candidate function  $\dot{V}_2$  in (37) is negative definite for  $\kappa_2$  greater than zero, the system is stable.

The performance of the two proposed controllers will be analyzed in the subsequent section for tracking the reference temperature in a realistic HVAC system for the Shifa International Hospital, Pakistan.

## 5. Simulation and Results

### 5.1. Environmental Conditions

Environmental conditions have a great influence on the power consumed by HVAC systems when achieving a desired setpoint. The difference in ambient temperature and the setpoint is directly proportional to the power consumed. Heat transfer takes place through the outer boundaries of the zone due to temperature differences, and the flow of heat flux increases with an increase in this difference, causing more power consumption by the HVAC system to keep tracking the desired setpoint. Three time spans have been considered to validate the performance of the proposed controllers. Global solar irradiation, wind speed, and ambient temperature data have been collected from [45], with a sampling period of 10 min, as shown in Figures 5–7, respectively. All of the simulation scenarios and controller designs have been carried out in MATLAB Simulink R2022b. The computer used has an Intel(R) Core(TM) i7-10850H CPU operating at 2.70 GHz, 2712 MHz, and having a total of 32 GB of installed physical memory.

Various phases of the year are considered to evaluate the controller performance under different environmental conditions and analyze the influence of weather conditions on the dynamic behavior of the zone temperature. The length of each phase is taken as a quarter of a year (approx. 112 days) to cover all the seasons in a year. To verify the robust response of the proposed controllers, the model has been tested against variations in environmental and in-room parameters. Variations in the required room temperatures and external parameters have been included in the validation process by considering three samples of environmental and operational procedure data from different time frames of a year. It can be observed from Figures 5–7 that the length of each span is 111.67 days.

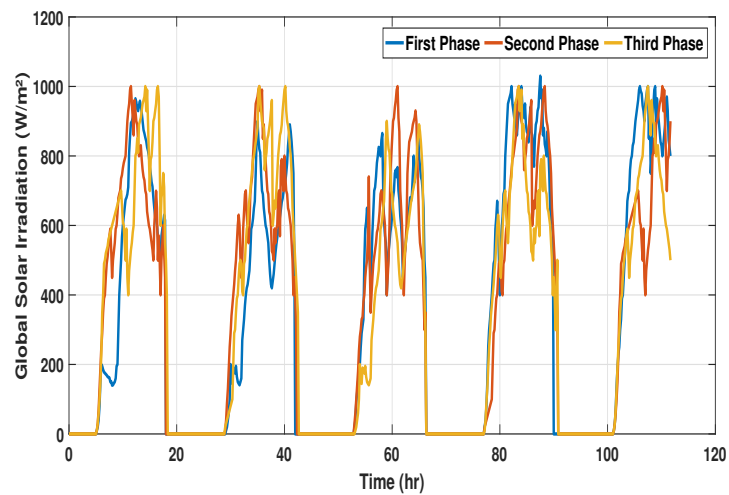


Figure 5. Global solar irradiation in all three time periods.

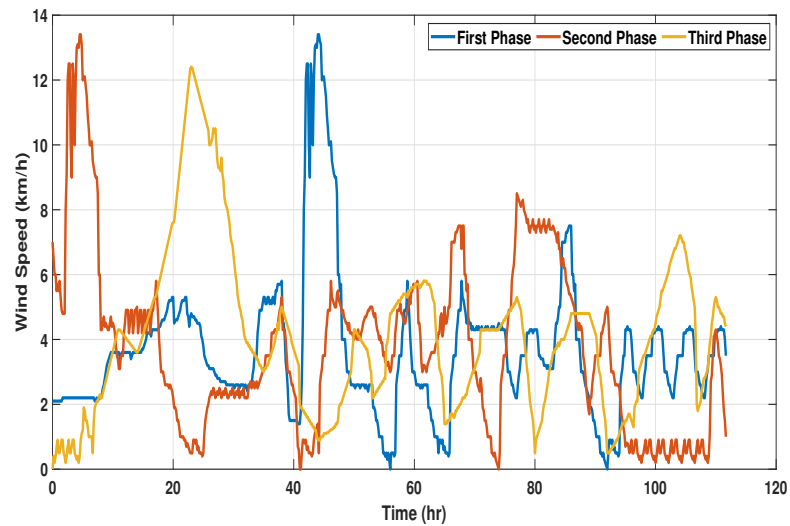


Figure 6. Wind speed in all three time periods.

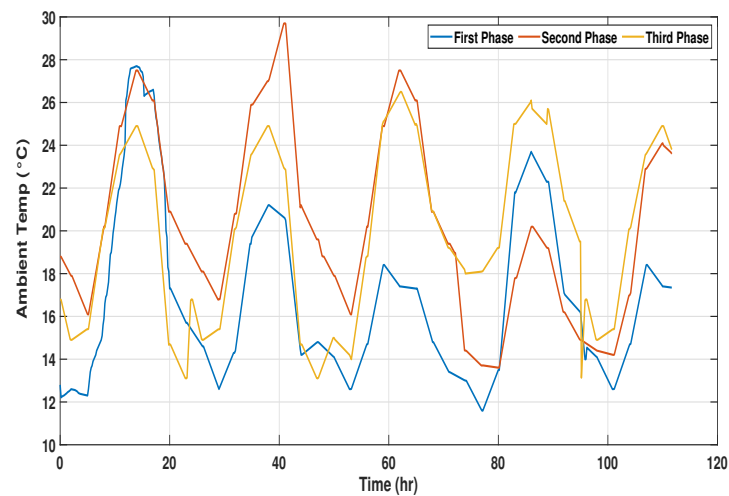


Figure 7. Outside ambient temperature in all three time periods.

### 5.2. Dynamic Setpoint

In the case of a hospital OT, the temperature setpoint is selected on the basis of the required operation procedure and the comfort of the patient. Research work is available in

the literature which deals with fixed setpoints [6]. This work shows overshoots and large settling times, which are not useful in the case of hospital OTs.

### 5.3. Johnson Temperature Controller

To gather experimental results, a Trane air cooled chiller plant was installed at the under-observation OT zone. The chiller was equipped with a built-in Johnson temperature controller (JTC) to track the desired zone setpoint. The data was recorded and the response of the JTC is presented in Figures 8–10 for all three time spans.

All three cases with JTC show identical responses against dynamic setpoints, where poor tracking performance and undesired oscillations are observed. Even a constant setpoint response shows a steady-state error with large harmonics, which is not suitable for clinical purposes. Large overshoots and undershoots in the zone temperature present unnecessary delays, as the environment is not suitable to initiate the operation. These delays in settling time and power steady-state response force delays in operation initiation that cause huge power losses. Sometimes during an operation, a quick change in zone temperature is required to make it feasible for the doctors and patients. The existing JTC controller appears not to be able to achieve such an abrupt change. A robust and smart controller is thus required which presents a fast dynamic response, less over/undershoots, a stable steady-state response, and a shorter settling time, ultimately leading to a decrease in the electric power consumed during large overshoots and oscillations.

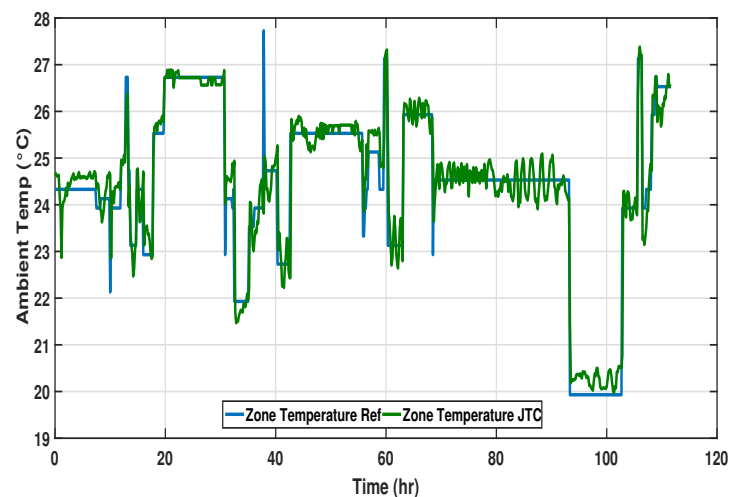


Figure 8. Zone temperature and its required reference for the first span of time using the JTC.

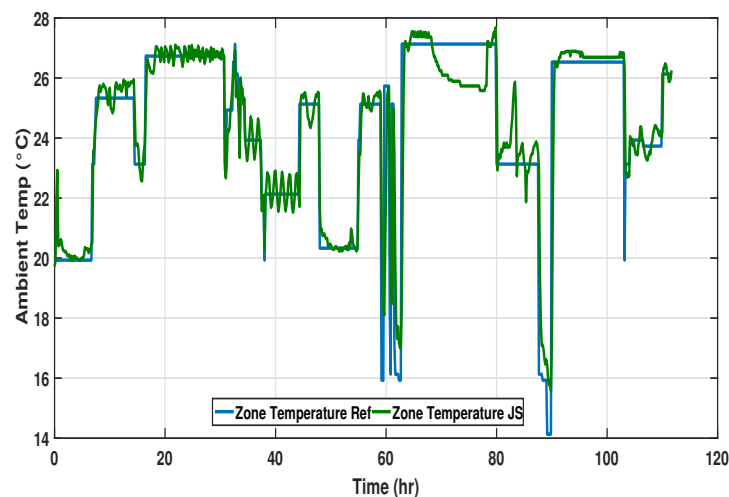


Figure 9. Zone temperature and its required reference for the second span of time using the JTC.

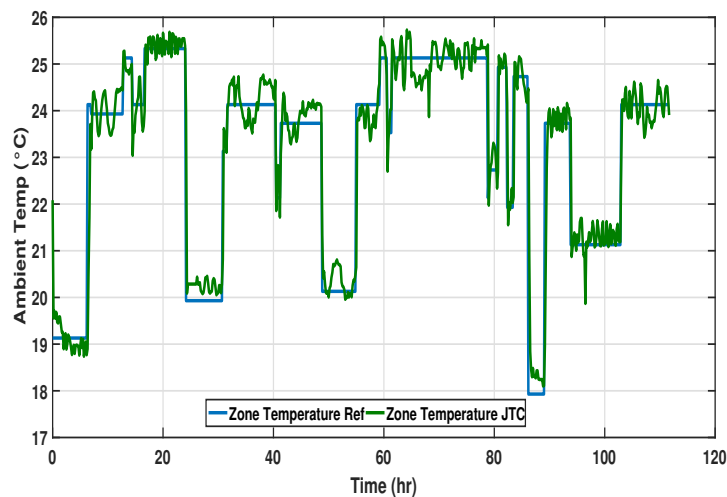


Figure 10. Zone temperature and its required reference for the third span of time using the JTC.

#### 5.4. Implementation of DISMC Temperature Controller

A DISMC for zone temperature control has been designed for tracking the dynamic zone temperature setpoint. The mathematical evaluation of DISMC has been presented in the controller design section. The performance of the controller is tested under the influence of weather conditions for all three time spans, with the results presented in Figures 11–13.

The system response during the second and third phases shows better results. The controller helps the HVAC system to track the desired reference in an effective way with zero steady-state error. It has been observed during all the phases that zone temperature sometimes takes up to half an hour to settle down to the required reference due to overshoots. However, the overshoots are not large, which leads to less power consumption and better zone temperature regulation.

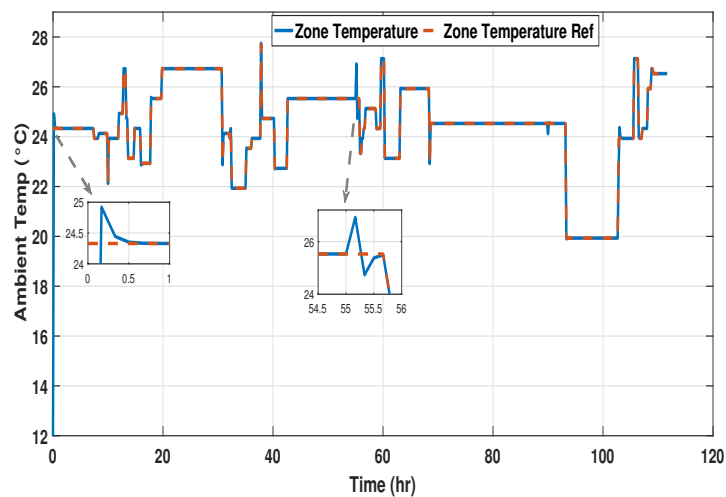


Figure 11. Zone temperature and its required reference for the first span of time using DISMC.

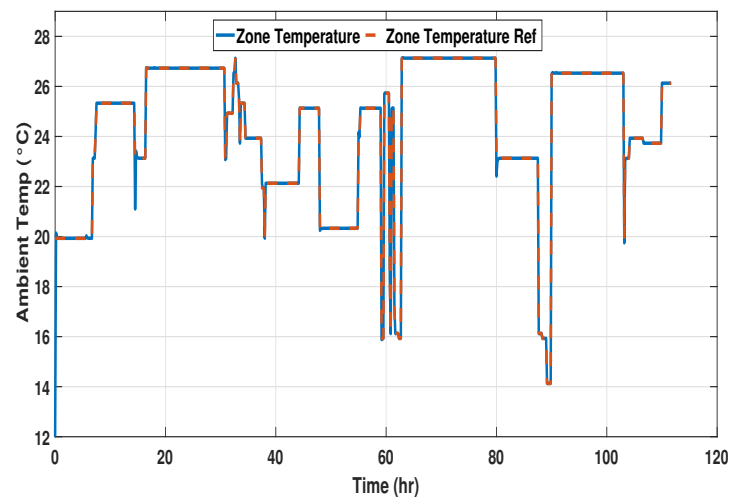


Figure 12. Zone temperature and its required reference for the second span of time using DISMC.

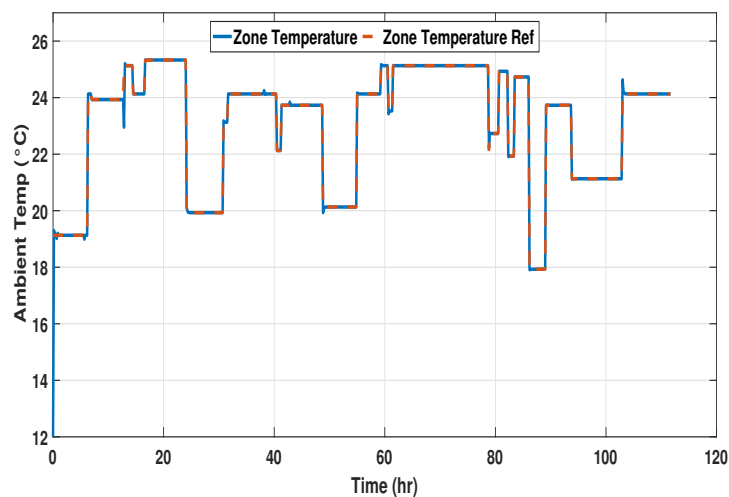


Figure 13. Zone temperature and its required reference for the third span of time using DISMC.

### 5.5. Implementation of ITSMC Temperature Controller

To further decrease the overshoots and to produce a better tracking response, the terminal part has been introduced in the controller design. The performance of the designed controller is evaluated by examining the response of the system under the same testing conditions as DISMC. The responses of ITSMC to the dynamic setpoints are presented in Figures 14–16.

During all three phases, the response is satisfactory, with zero overshoots and a small settling time, making it an ideal controller for OT zone temperature control. With negligible overshoot, a small settling time, and negligible steady-state error, the proposed ITSMC controller helps to prepare the OT quickly for the next procedure and supports abrupt temperature variations.

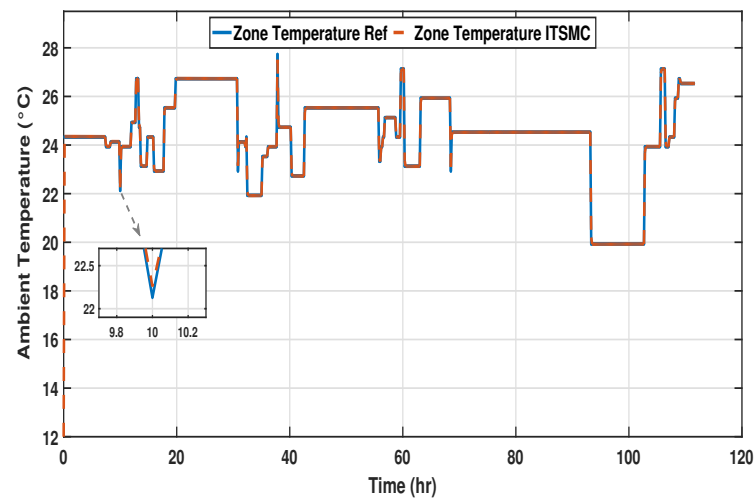


Figure 14. Zone temperature and its required reference for the first span of time using ITSMC.

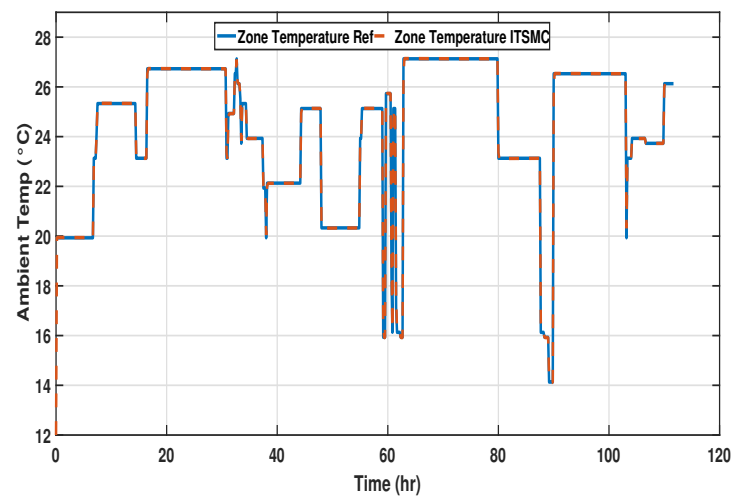


Figure 15. Zone temperature and its required reference for the second span of time using ITSMC.

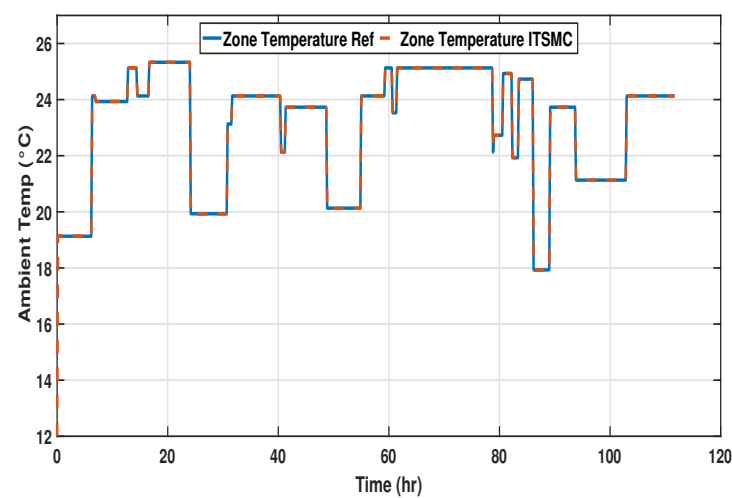


Figure 16. Zone temperature and its required reference for the third span of time using ITSMC.

### 5.6. Comparative Analysis

A comparative performance analysis of JTC and the proposed two controllers is established in this section. The performance of the proposed DISMC and ITSMC temperature

controllers with installed JTC for tracking the desired dynamic setpoints in all three phases are presented in Figures 17–19.

It can be seen that DISMC shows an overshoot of 0.5 °C at the first phase to the desired reference and takes up to half an hour to reach the desired reference, whereas ITSMC has zero overshoot and a smaller settling time. After 55 hr of observation, a large overshoot of 2 degrees Celsius is seen in DISMC, which forces a delay of half an hour to initiate the procedure so that the system can settle down to the desired reference. At each large transition, DISMC shows overshoots that are not suitable for the clinical installation, whereas ITSMC shows satisfactory results, which makes it a better choice for zone temperature controllers in the case of an operation theater. The JTC, on the other hand, presents significant oscillations and steady-state errors. A similar overshoot in the zone temperature has been observed in the other two observation phases with the DISMC temperature regulator, whereas the ITSMC temperature controller shows promising results with negligible overshoot, a small settling time, and zero steady-state error.

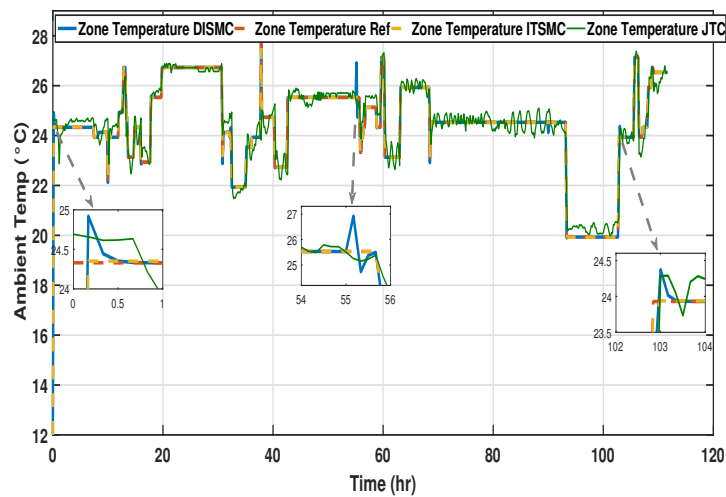


Figure 17. Comparative analysis of zone temperature in the case of JTC, DISMC, and ITSMC in the first span of time.

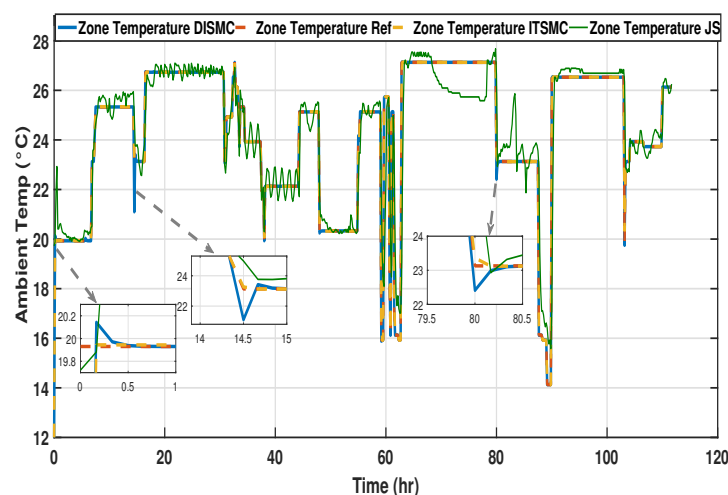
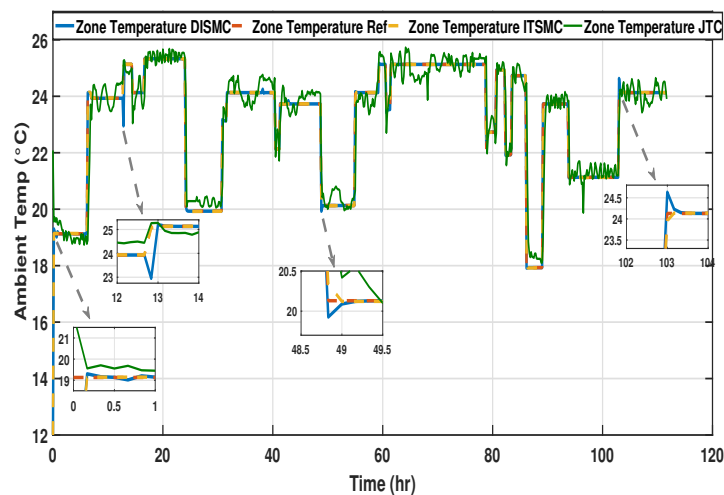
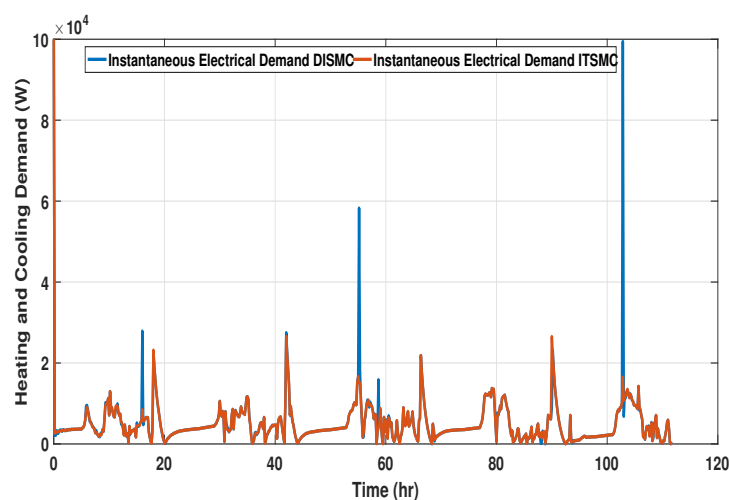


Figure 18. Comparative analysis of zone temperature in the case of JTC, DISMC, and ITSMC in the second span of time.



**Figure 19.** Comparative analysis of zone temperature in the case of JTC, DISMC, and ITSMC in the third span of time.

A comparative analysis of the instantaneous power consumption in each observation phase by the HVAC system using DISMC and ITSMC is presented in Figures 20–22, respectively. For phase one, large spikes in power consumption are observed during the temperature setpoints transition in the case of DISMC, whereas the spikes in instantaneous power demand in the case of ITSMC are small. Similar behavior is recorded in the second and third phases of the observation period. For DISMC, large spikes occur at the transition point in the dynamic setpoint of zone temperature. The HVAC system tries to attain the required zone temperature but DISMC overshoots. The accumulative power consumed during each observation phase has been evaluated to analyze the total power consumed by the HVAC system in the case of the DISMC and ITSMC-based controllers. The accumulative power consumed by the HVAC system in the first, second, and third phases are shown in Figures 23–25, respectively. The energy consumed by the HVAC operation is dependent on the instantaneous power of the hospital OT unit over the time periods of HVAC operation. Thus, increasing the working period or the demanded power would increase the energy consumption.



**Figure 20.** Comparative analysis of power consumption with the DISMC and ITSMC temperature regulators during the first span of time.

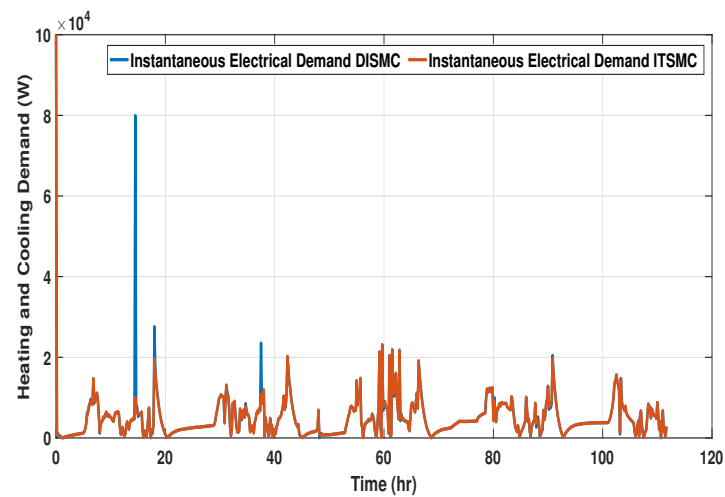


**Figure 21.** Comparative analysis of power consumption with the DISMC and ITSMC temperature regulators during the second span of time.

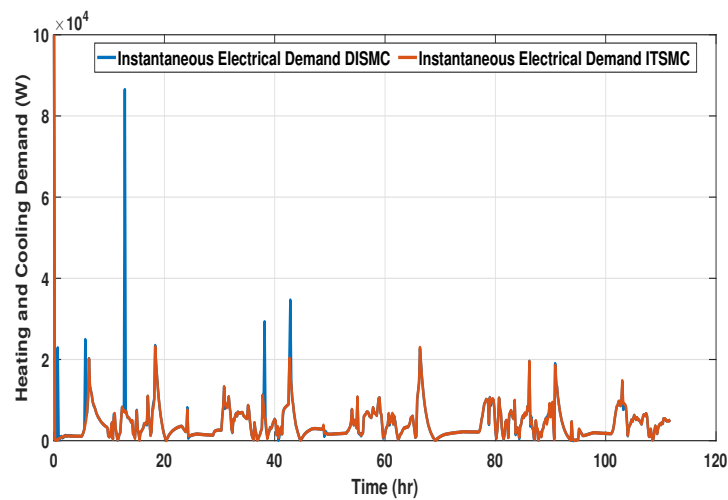


**Figure 22.** Comparative analysis of power consumption with the DISMC and ITSMC temperature regulators during the third span of time.

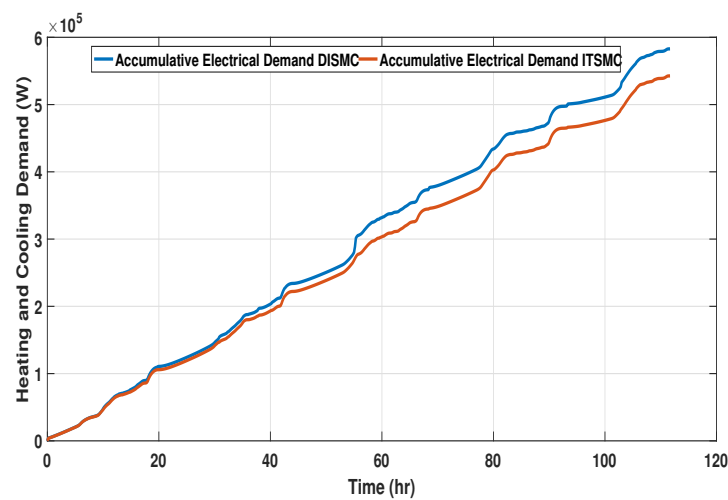


**Figure 23.** Comparative analysis of total power consumption by the HVAC during the first phase of observation.

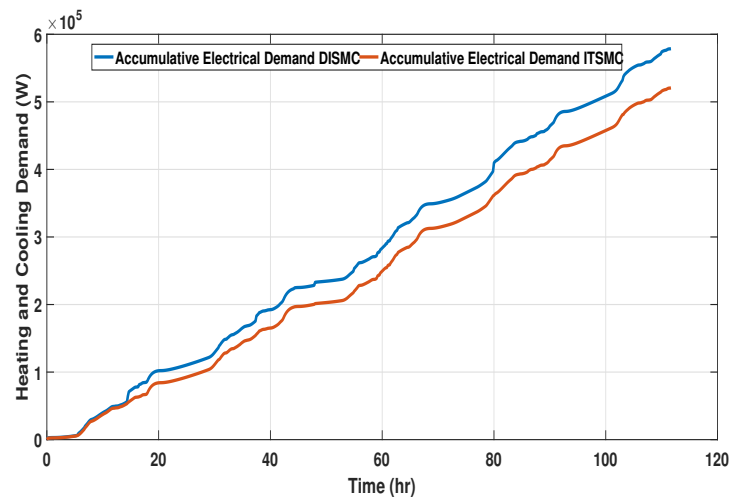


**Figure 24.** Comparative analysis of total power consumption by the HVAC during the second phase of observation.

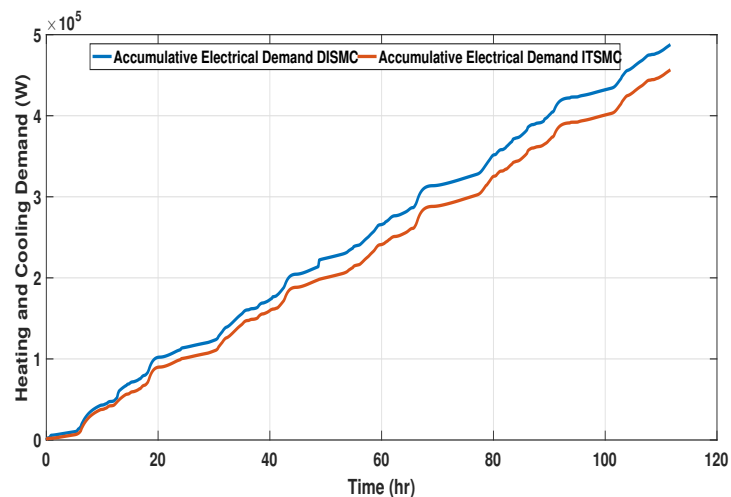


**Figure 25.** Comparative analysis of total power consumption by the HVAC during the third phase of observation.

It can be observed that a larger amount of accumulative power is consumed by the HVAC system in the case of DISMC installation. This rise in consumed power is due to an overshoot observed in the instantaneous power consumption at setpoint transitions. While the power consumed by the HVAC system with the ITSMC temperature regulator is low, which shows its economic benefits due to smooth and better control actions.

Better performance in achieving the desired temperature, and less consumption by the ITSMC compared to DISMC, shows the advantages of using a better controller with precise control actions.

## 6. Conclusions

This paper proposes two nonlinear controllers, DISMC and ITSMC, for the temperature dynamic setpoint regulation in a controlled temperature environment for OT and ICT extreme health care units. A realistic scenario of a hospital OT is considered for evaluating their responses and performance in achieving desired temperature setpoints. During the performance analysis, it has been evaluated that the proposed controllers perform better than the already installed Johnson temperature controller. Large oscillations around the dynamic setpoints and high SSE throughout all of the three observation spans have been seen in the case of the JTC. The issues of continuous oscillations and SSE have been resolved with the implementation of DISMC and ITSMC. During comparative analysis, it

has been observed that DISMC produces larger overshoot in the zone temperature from the setpoint at each transition of dynamic zone temperature setpoints, whereas, ITSMC shows negligible overshoot. Subsequently, zone temperature overshoot ( $0.5^0$ ) with the DISMC regulator consumes more time and electrical power to settle down to the required setpoint, which affects the time and energy efficiency of any clinical procedure, while the power consumed by the HVAC system with the ITSMC temperature regulator is low. This points to the performance and economic superiority of ITSMC for OT zone temperature regulation, and thus it is a more practical controller for such a critical application. This work can be extended to all other living zones such as cafeterias, offices, private rooms, ICUs, and general wards. Furthermore, it can also be extended to control the zone temperature of incubators in any hatchery.

**Author Contributions:** Conceptualization, A.H., M.U. and I.A.; methodology, A.H. and M.U.; software, A.H. and M.U.; validation, A.H., M.U. and I.A.; formal analysis, A.H. and M.U.; investigation, A.H., M.U., I.A., and K.S.; resources, I.A., and K.S.; data curation, M.U.; writing—original draft preparation, A.H.; writing—review and editing, I.A., K.S. and Z.A.; visualization, A.H. and M.U.; supervision, I.A. and Z.A.; project administration, I.A. and Z.A.; funding acquisition, Z.A. All authors have read and agreed to the published version of the manuscript.

**Funding:** This research received no external funding.

**Institutional Review Board Statement:** Not applicable

**Informed Consent Statement:** Not applicable

**Data Availability Statement:** Not applicable

**Acknowledgments:** Thanks to the School of Engineering, London South Bank University in providing resources for PhD studies.

**Conflicts of Interest:** The authors declare no conflict of interest.

## Nomenclature

### List of Abbreviations

|       |  |
|-------|--|
| S     | Sliding manifold                           |
| ANN   | Artificial neural network                  |
| DISMC | Double integral sliding mode control       |
| EUI   | Energy use intensity                       |
| HVAC  | Heating, ventilation, and air conditioning |
| ICT   | Islamabad Capital Territory                |
| IEA   | International Energy Agency                |
| ITSMC | Integral terminal sliding mode control     |
| JCI   | Joint Commission International             |
| JTC   | Johnson temperature controller             |
| MIMO  | Multi input multi output                   |
| MPC   | Model predictive control                   |
| OR    | Operation room                             |
| OT    | Operation theater                          |
| S/V   | Surface-to-volume                          |
| SIH   | Shifa International Hospital               |
| SMC   | Sliding mode control                       |
| SSE   | Steady-state error                         |
| V     | Lyapunov candidate function                |
| ZN    | Ziegler–Nichols                            |

**List of Symbols**

|                              |   |
|------------------------------|---|
| $R_{win.j}$                  | Window resistance ( $KW^{-1}$ )   |
| $a_1, a_2, a_3$              | Sliding coefficients  |
| $e_1, e_2, e_3, e_5$         | Errors  |
| $T_{OR_{ref}}$               | OR temperature reference ( $^{\circ}C$ )                                      |
| $\alpha$                     | Unit between 0 and 1  |
| $\dot{q}_{wi.j}$             | The flow of heat flux from the internal layer towards the wall node (W)       |
| $\dot{v}_a$                  | Volume of air conditioned per minute ( $m^3/min$ )                            |
| $\dot{x}_{hs}, \dot{x}_{cs}$ | Heating/cooling input thermal power (W)                                       |
| $\dot{x}_{is}$               | Internal free heat gain due to person and equipment (W)                       |
| $\dot{x}_{sg}$               | Thermal energy contribution due to solar radiation                            |
| $\dot{x}_v$                  | Heat transfer through the windows due to ventilation (W)                      |
| $\dot{x}_{we.j}$             | The flow of heat flux from the external layer towards the wall node (W)       |
| $\dot{x}_{win}$              | Flow of heat charge across the window (W)                                     |
| $\dot{x}_{wl}$               | Heat transfer to the wall (W)   |
| $\kappa_2$                   | Design parameter of sliding manifold  |
| $\lambda_2$                  | Positive constant   |
| $\phi$                       | Small number used to reduce chattering  |
| $\psi_{fl}$                  | Absorption coefficient  |
| $\psi_{w.j}$                 | Wall absorbance coefficient   |
| $\rho_v, c_a$                | The density ( $kg\ m^{-3}$ ) and specific heat of the air ( $kJ/kg \cdot K$ ) |
| $\tau_{win.j}$               | Transmittance coefficient of the window glass ( $Wm^2\ K^{-1}$ )              |
| $C_{OR}$                     | Total capacitance of OR ( $JK^{-1}$ )   |
| $c_{vv}$                     | Specific heat of air ventilated from the system ( $kJ/kg \cdot K$ )           |
| $C_{w.j}$                    | Total thermal capacitance of the wall ( $JK^{-1}$ )                           |
| $f_j$                        | Function of shadow on the window  |
| $I_{jn}$                     | Amount of solar irradiation ( $Wm^2$ )  |
| $M_v$                        | Mass of air ventilated from the system (g/mol)                                |
| $S_{w.j}$                    | Total opaque surface area of wall ( $m^2$ )                                   |
| $S_{win.j}$                  | Total transparent surface area of the window ( $m^2$ )                        |
| $T_{OR}$                     | OR Internal air temperature ( $^{\circ}C$ )                                   |
| $T_v$                        | Temperature of ventilation system ( $^{\circ}C$ )                             |
| $T_{w.j}$                    | Temperature of wall internal node ( $^{\circ}C$ )                             |
| $U_v$                        | Overall heat transfer coefficient ( $Wm^2\ K^{-1}$ )                          |

Appendix A

BLOCK E-2 (FIRST FLOOR)

| DEPARTMENT OCCUPATION | AREA      |
|-----------------------|-----------|
| OR PLAN E-2           | 14133 Sft |
| MAINTENANCE DEPT.     | 1319 Sft  |
| CSSD                  | 4551 Sft  |
|                       |           |

OR PLAN E-2  
14133Sft

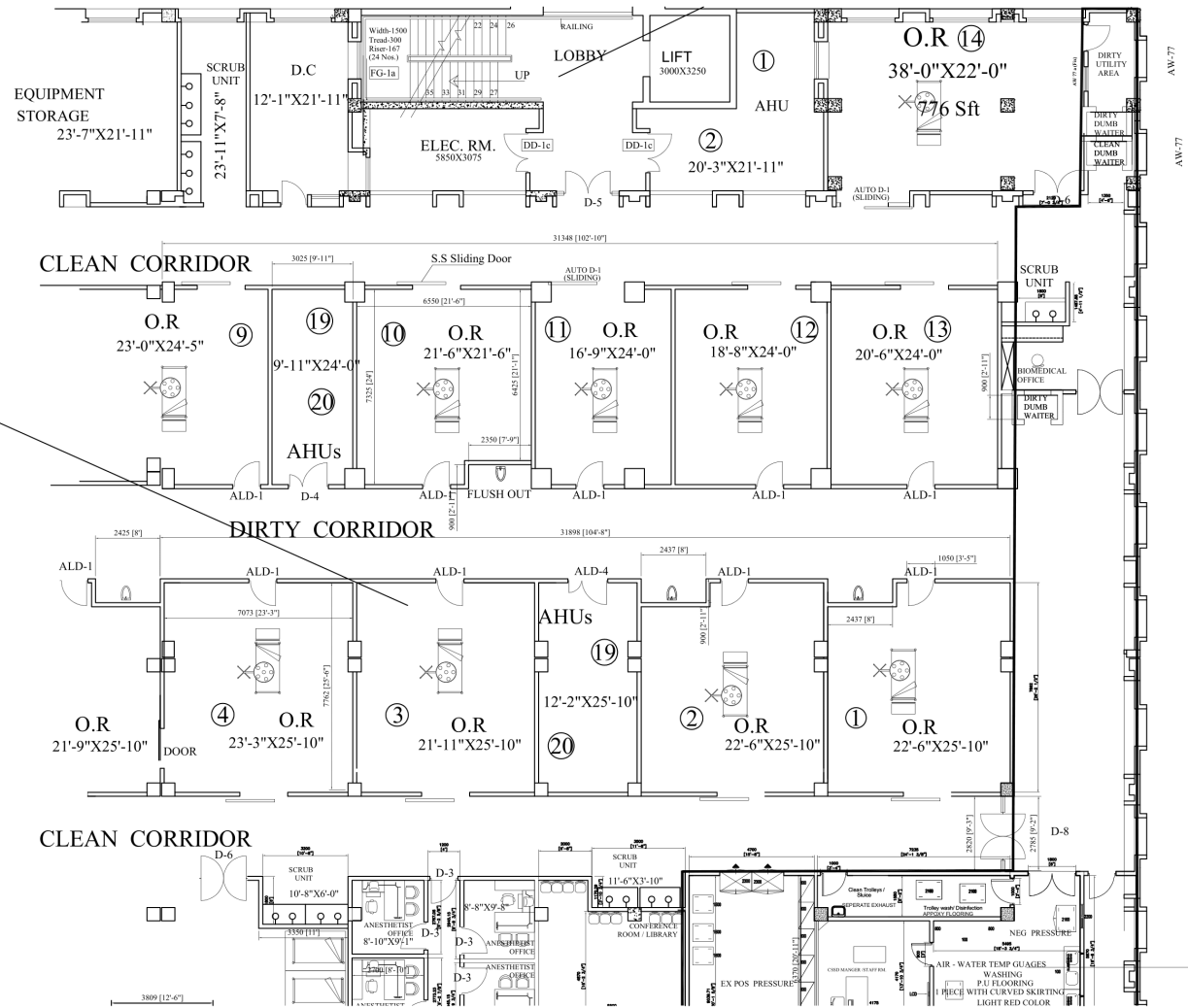


Figure A1. OR section layout.

## References

1. Ding, Y.; Zhang, Q.; Yuan, T.; Yang, K. Model input selection for building heating load prediction: A case study for an office building in Tianjin. *Energy Build.* **2018**, *159*, 254–270. [\[CrossRef\]](#)
2. Hietaharju, P.; Ruusunen, M.; Leiviskä, K. A dynamic model for indoor temperature prediction in buildings. *Energies* **2018**, *11*, 1477. [\[CrossRef\]](#)
3. Perera, D.W.U.; Pfeiffer, C.F.; Skeie, N.O. Modelling the heat dynamics of a residential building unit: Application to Norwegian buildings. *Model. Identif. Control J.* **2014**, *35*, 43–57. [\[CrossRef\]](#)
4. Rousselot, M. Energy efficiency trends in buildings. *Odyssee-Mure* **2018**, *4*, 1–4.
5. Costa, A.; Keane, M.M.; Torrens, J.I.; Corry, E. Building operation and energy performance: Monitoring, analysis and optimisation toolkit. *Appl. Energy* **2013**, *101*, 310–316. [\[CrossRef\]](#)
6. Adegbenro, A.; Short, M.; Angione, C. An integrated approach to adaptive control and supervisory optimisation of HVAC control systems for demand response applications. *Energies* **2021**, *14*, 2078. [\[CrossRef\]](#)
7. Pedersen, L. Use of different methodologies for thermal load and energy estimations in buildings including meteorological and sociological input parameters. *Renew. Sustain. Energy Rev.* **2007**, *11*, 998–1007. [\[CrossRef\]](#)
8. Fateh, A.; Borelli, D.; Spoladore, A.; Devia, F. A state-space analysis of a single zone building considering solar radiation, internal radiation, and PCM effects. *Appl. Sci.* **2019**, *9*, 832. [\[CrossRef\]](#)
9. Malinowski, A.; Muzychak, A. Mathematical modeling of the building thermal state taking into account the heat and energy impact of the environment. In Proceedings of the IOP Conference Series: Materials Science and Engineering, Yekaterinburg, Russia, 13–16 November 2017; IOP Publishing: Bristol, UK, 2018; Volume 415, p. 012047.
10. Amara, F.; Agbossou, K.; Cardenas, A.; Dubé, Y.; Kelouwani, S. Comparison and simulation of building thermal models for effective energy management. *Smart Grid Renew. Energy* **2015**, *6*, 95. [\[CrossRef\]](#)
11. Ljung, L. *System Identification: Theory for the User*; Pearson: London, UK, 1998; pp. 163–173.
12. Lebrun, J. Simulation of a HVAC system with the help of an engineering equation solver. In Proceedings of the Seventh International IBPSA Conference, Rio de Janeiro, Brazil, 13–15 August 2001; pp. 13–15.
13. Kato, K.; Sakawa, M.; Ishimaru, K.; Ushiro, S.; Shibano, T. Heat load prediction through recurrent neural network in district heating and cooling systems. In Proceedings of the 2008 IEEE International Conference on Systems, Man and Cybernetics, Singapore, 12–15 October 2008; pp. 1401–1406.
14. Heiselberg, P.K. The Energy Performance Assessment of nZEBs: Limitations of the Quasi-Steady State Approach. In Proceedings of the CLIMA 2016—12th REHVA World Congress, Aalborg, Denmark, 22–25 May 2016.
15. Mahdavi, A.; Tahmasebi, F.; Kayalar, M. Prediction of plug loads in office buildings: Simplified and probabilistic methods. *Energy Build.* **2016**, *129*, 322–329. [\[CrossRef\]](#)
16. Paolini, R.; Zani, A.; MeshkinKiya, M.; Castaldo, V.L.; Pisello, A.L.; Antretter, F.; Poli, T.; Cotana, F. The hygrothermal performance of residential buildings at urban and rural sites: Sensible and latent energy loads and indoor environmental conditions. *Energy Build.* **2017**, *152*, 792–803. [\[CrossRef\]](#)
17. Yang, L.; Lam, J.C.; Tsang, C.L. Energy performance of building envelopes in different climate zones in China. *Appl. Energy* **2008**, *85*, 800–817. [\[CrossRef\]](#)
18. Handbook-Fundamentals, A.; Edition, S. *Inc.*; See Page 14.14 for Summary Description of RP-1171 Work on Uncertainty in Design Temperatures; American Society of Heating, Refrigerating and Air-Conditioning Engineers: Atlanta, GA, USA, 2009.
19. De Rosa, M.; Bianco, V.; Scarpa, F.; Tagliafico, L.A. Heating and cooling building energy demand evaluation; a simplified model and a modified degree days approach. *Appl. Energy* **2014**, *128*, 217–229. [\[CrossRef\]](#)
20. Kramer, R.; Van Schijndel, J.; Schellen, H. Simplified thermal and hygric building models: A literature review. *Front. Archit. Res.* **2012**, *1*, 318–325. [\[CrossRef\]](#)
21. Crawley, D.B.; Hand, J.W.; Kummert, M.; Griffith, B.T. Contrasting the capabilities of building energy performance simulation programs. *Build. Environ.* **2008**, *43*, 661–673. [\[CrossRef\]](#)
22. Naidu, D.S.; Rieger, C.G. Advanced control strategies for heating, ventilation, air-conditioning, and refrigeration systems—An overview: Part I: Hard control. *Hvac&R Res.* **2011**, *17*, 2–21.
23. Tashtoush, B.; Molhim, M.; Al-Rousan, M. Dynamic model of an HVAC system for control analysis. *Energy* **2005**, *30*, 1729–1745. [\[CrossRef\]](#)
24. Anderson, M.; Buehner, M.; Young, P.; Hittle, D.; Anderson, C.; Tu, J.; Hodgson, D. MIMO robust control for HVAC systems. *IEEE Trans. Control Syst. Technol.* **2008**, *16*, 475–483. [\[CrossRef\]](#)
25. Avci, M.; Erkoc, M.; Rahmani, A.; Asfour, S. Model predictive HVAC load control in buildings using real-time electricity pricing. *Energy Build.* **2013**, *60*, 199–209. [\[CrossRef\]](#)
26. West, S.R.; Ward, J.K.; Wall, J. Trial results from a model predictive control and optimisation system for commercial building HVAC. *Energy Build.* **2014**, *72*, 271–279. [\[CrossRef\]](#)
27. Široký, J.; Oldewurtel, F.; Cigler, J.; Prívvara, S. Experimental analysis of model predictive control for an energy efficient building heating system. *Appl. Energy* **2011**, *88*, 3079–3087. [\[CrossRef\]](#)
28. Afram, A.; Janabi-Sharifi, F. Theory and applications of HVAC control systems—A review of model predictive control (MPC). *Build. Environ.* **2014**, *72*, 343–355. [\[CrossRef\]](#)

29. Kreider, J.; Claridge, D.; Curtiss, P.; Dodier, R.; Haberl, J.; Krarti, M. Building energy use prediction and system identification using recurrent neural networks. *J. Sol. Energy Eng. Aug.* **1995**, *117*, 161–166. [[CrossRef](#)]
30. Kalogirou, S.; Neocleous, C.; Schizas, C. Building heating load estimation using artificial neural networks. In Proceedings of the 17th International Conference on Parallel Architectures and Compilation Techniques, San Francisco, CA, USA, 11–15 October 1997; Volume 8, p. 14.
31. Lei, J.; Hongli, L.; Cai, W. Model predictive control based on fuzzy linearization technique for HVAC systems temperature control. In Proceedings of the 2006 1ST IEEE Conference on Industrial Electronics and Applications, Singapore, 24–26 May 2006; pp. 1–5.
32. Wang, J.; An, D.; Lou, C. Application of fuzzy-PID controller in heating ventilating and air-conditioning system. In Proceedings of the 2006 International Conference on Mechatronics and Automation, Luoyang, China, 25–28 June 2006; pp. 2217–2222.
33. Basin, M.V.; Ramírez, P.C.R. A supertwisting algorithm for systems of dimension more than one. *IEEE Trans. Ind. Electron.* **2014**, *61*, 6472–6480. [[CrossRef](#)]
34. Shah, A.; Huang, D.; Huang, T.; Farid, U. Optimization of building energy consumption by designing sliding mode control for multizone VAV air conditioning systems. *Energies* **2018**, *11*, 2911. [[CrossRef](#)]
35. Shah, A.; Huang, D.; Chen, Y.; Kang, X.; Qin, N. Robust sliding mode control of air handling unit for energy efficiency enhancement. *Energies* **2017**, *10*, 1815. [[CrossRef](#)]
36. Gonzalez, T.; Moreno, J.A.; Fridman, L. Variable gain super-twisting sliding mode control. *IEEE Trans. Autom. Control* **2011**, *57*, 2100–2105. [[CrossRef](#)]
37. Wang, Z.; Bao, W.; Li, H. Second-order dynamic sliding-mode control for nonminimum phase underactuated hypersonic vehicles. *IEEE Trans. Ind. Electron.* **2016**, *64*, 3105–3112. [[CrossRef](#)]
38. Borowski, M.; Mazur, P.; Kleszcz, S.; Zwolińska, K. Energy monitoring in a heating and cooling system in a building based on the example of the Turówka hotel. *Energies* **2020**, *13*, 1968. [[CrossRef](#)]
39. Coraci, D.; Brandi, S.; Piscitelli, M.S.; Capozzoli, A. Online implementation of a soft actor-critic agent to enhance indoor temperature control and energy efficiency in buildings. *Energies* **2021**, *14*, 997. [[CrossRef](#)]
40. Espejel-Blanco, D.F.; Hoyo-Montaño, J.A.; Arau, J.; Valencia-Palomo, G.; García-Barrientos, A.; Hernández-De-León, H.R.; Camas-Anzueto, J.L. HVAC control system using predicted mean vote index for energy savings in buildings. *Buildings* **2022**, *12*, 38. [[CrossRef](#)]
41. Hu, S.; Chen, J.; Chuah, Y. Energy cost and consumption in a large acute hospital. *Int. J. Archit. Sci.* **2004**, *5*, 11–19.
42. Khalil, H.K. *Nonlinear Systems*; Patience Hall: Upper Saddle River, NJ, USA, 2002.
43. Qureshi, M.A.; Ahmad, I.; Munir, M.F. Double integral sliding mode control of continuous gain four quadrant quasi-Z-source converter. *IEEE Access* **2018**, *6*, 77785–77795. [[CrossRef](#)]
44. Pradhan, R.; Subudhi, B. Double integral sliding mode MPPT control of a photovoltaic system. *IEEE Trans. Control Syst. Technol.* **2015**, *24*, 285–292. [[CrossRef](#)]
45. Pakistan Meteorological Department. National Weather Forecasting Centre, Islamabad. Available online: <https://nwfc.pmd.gov.pk/new/daily-forecast-en.php> (accessed on 5 January 2023).

**Disclaimer/Publisher’s Note:** The statements, opinions and data contained in all publications are solely those of the individual author(s) and contributor(s) and not of MDPI and/or the editor(s). MDPI and/or the editor(s) disclaim responsibility for any injury to people or property resulting from any ideas, methods, instructions or products referred to in the content.